Available online at www.sciencedirect.com
ScienceDirect
Catalysis Today 122 (2007) 168–177
CATALYSIS TODAY
www.elsevier.com/locate/cattod

Kinetics of the photocatalytic degradation of benzene

N. Doucet, O. Zahraa *, M. Bouchy

Département de Chimie Physique des Réactions-UMR 7630 CNRS-INPL, ENSIC, 1 rue Grandville, BP 20451, F-54001 Nancy Cedex, France

Available online 30 January 2007

Abstract

The kinetics of photocatalytic degradation of benzene in air has been studied on a standardized micro-pilot scale continuous flow apparatus. Both the yield of conversion of the reactant and the apparition of CO and CO_2 have been monitored. The influences of concentration, light flux and temperature on the initial degradation rate have been studied. An apparent deactivation of the catalyst was identified as the formation of a resistant intermediate, which underwent a slow photocatalytic degradation leading to CO and CO_2 as the main carbonaceous products of oxidation. A kinetic model has been derived which gives a satisfactory agreement with the experiments. The relative humidity is not of importance in the primary attack of benzene but it is of great importance in the degradation reaction. Increasing the relative humidity indeed allowed the conversion yield to be much increased due to acceleration in the degradation of the intermediate.

Keywords: Photocatalysis; Pollution; Benzene; Kinetics; Reactor

1. Introduction

Benzene ranks amongst the common and harmful VOCs and its presence in the air is to be eliminated in order to protect the environment. In this respect, advanced oxidation processes (AOP) [1], prove very efficient for organic micropollutants. These techniques aim at the production of the hydroxyl radical OH° which is a powerful enough oxidant to lead to a full mineralization of most of VOCs in the presence of oxygen. In particular, photocatalysis [2,3], which belongs to AOPs, has proved very effective in environmental destruction of VOCs [4] especially in the case of benzene [5–13]. The purpose of the present study is to use a standardized photocatalytic reactor in order to investigate the photocatalytic degradation of benzene and to collect experimental data necessary for the design of a photocatalytic reactor for the treatment of polluted air. This implies the determination of the intrinsic rate and the effect of various experimental conditions on the kinetics [5].

2. Experimental

2.1. Experimental set-up

The experimental set-up shown in Fig. 1 has been described in detail in an earlier study [14]. It consists in a continuous flow annular reactor equipped with a chromatographic analysis.

An atmospheric airflow provided by a compressor was allowed to flow through a set of two traps composed of 400 mL calcium sulphate (elimination of water vapour traces) and 400 mL molecular sieve 5 Å (CO_2 and organics adsorption). The dry and pure airflow obtained was then split into three paths for the preparation of the reactor feed. The molar flow rate of air was finely controlled in each path by a digital mass flow regulator. The three paths were equipped with check valves to prevent back mixing, and with relief valves in order to prevent an accidental overpressure in the Pyrex vessels. The first and second paths were used for benzene and water supplies, both working on the same principle. Air was allowed to bubble through a sintered Pyrex glass tube in the pure liquid maintained under strong agitation in a thermostatic bath, so that the air was saturated with the compound at the bath temperature before leaving the bubbler. This system allowed us to set the total volume flow rate Q, the benzene molar fraction C (ppm) and the relative humidity H (%) by a careful adjustment

* Corresponding author. Tel.: +33 3 83175118; fax: +33 3 83378120.
E-mail address: Orfan.Zahraa@ensic.inpl-nancy.fr (O. Zahraa).

0920-5861/$ – see front matter © 2007 Elsevier B.V. All rights reserved.
doi:10.1016/j.cattod.2007.01.023

Nomenclature

$A(\theta)$	periphery of aggregates per unit of surface area (m^{-1})
C	molar fraction of benzene at the reactor entrance (ppm)
C_{CO}	molar fraction of CO (ppm)
C_{CO_2}	molar fraction of CO_2 (ppm)
$C(l,t)$	current molar fraction of benzene (ppm)
C_W	water concentration
F°	total incident light flux (photons mol cm^{-2} s^{-1})
F_E	molar flow rate at the reactor entrance (mol s^{-1})
H	relative humidity (%)
I_B	integral of the molar fraction of benzene disappeared for the deactivation phase
$I_{CO_x}(D)$	integral of the molar fraction of CO and CO_2 for the deactivation phase
$I_{CO_x}(R)$	integral of the molar fraction of CO and CO_2 for the regeneration phase
k_B	rate constant of the primary attack of benzene (turn-over number) (min^{-1})
k_{deg}	kinetic constant (mol min^{-1} m^{-2})
K_{LH}	Langmuir Hinshelwood benzene adsorption constant (ppm^{-1})
K_W	adsorption constant of water (ppm^{-1})
l	current length (m)
l°	length of the reactor (m)
Q	total flow rate (ml min^{-1})
r	reaction rate (mol min^{-1} m^{-2})
r_B	reaction rate of benzene for a clean surface (turn-over number) (min^{-1})
r_g	rate of germination (min^{-1} m^{-2})
r_I	degradation rate of the intermediate (turn-over number) (min^{-1})
S	catalyst support apparent surface area (m^2)
t	current time (s)
X	conversion yield
Z	total number of sites on the catalyst (mol)

Greek letters

θ_I	surface coverage of the sites by the deactivation species
ν_{B,CO_x}	stoichiometric coefficient of CO_x produce in the reaction degradation of the benzene
ν_{I,CO_x}	stoichiometric coefficient of CO_x produce in the reaction degradation of the intermediate

of the air flow rate in each of the three paths and the temperature in both bubblers [14].

The system used an annular reactor (see cross section in Fig. 2) equipped with four inlets and four outlets so as to ensure a good flow distribution. Experiments of residence time distribution, using a burst of ozone detected at the exit by photometry, revealed a hydrodynamic flow close to that of a plug flow reactor (PFR). As an example, the analysis of input and output signals for a volume flow rate of 200 mL min^{-1} given in Fig. 3 led to assimilate the reactor to a cascade of about 40 elementary perfectly stirred reactors; it is generally accepted that above a number of 20 elementary reactors, the experimental reactor can be considered practically as a PFR. The catalyst was washcoated on a fibreglass mat, which was placed between two Pyrex glass tubes in order to obtain the best contact between air and catalyst. The total mass of deposited catalyst was 600 mg. The central position of the lamp offered the best conditions for collecting the emitted photon flux. It was cooled by air being allowed to flow freely within a surrounding void space. A liquid section separated the lamp and the catalyst in order to control the temperature. The total diameter of the apparatus was 52 mm, and the mat fibreglass apparent area exposed to light was 300 cm^2.

2.2. Photocatalyst

The deposition of the catalyst followed a protocol defined in a previous work [15]. Degussa P25 was used as the catalyst. It was dispersed as a dilute aqueous suspension in the presence of nitric acid 10^{-3} M, which prevented titanium dioxide to aggregate during the mixing of the suspension. The fibreglass support was then impregnated, allowing an exact amount of catalyst to be deposited. After total evaporation of water the support was dried at 100 °C for 1 h and fired at 475 °C for 4 h in order to ensure a good adherence between catalyst and support by formation of siloxane bonds.

The absorption properties of the catalyst could not be measured by spectrophotometry due to the non-homogeneous nature of the support. However, the absorption was verified to be nearly total.

Samples of catalyst coated fibreglass have been controlled by optical and electron microscopy as shown in Fig. 4. Fig. 4a represents the impregnated support, which consists in a mat of thickness 1.8 mm, made of randomly oriented fibre bundles of rectangular section 300 μm × 40 μm. These bundles are made of actual fibres of diameter about 15 μm, as shown in Fig. 4b, on which catalyst crystals are fixed.

2.3. Analytical method

A continuous flow reactor was used so as to reach a stationary state. FID chromatography was chosen for the detection, using a filled column. A sampling system made use of a six-way valve permitting to fill the sampling loop either by the entrance or by the exit flow, without altering the feed of the reactor. The conversion X was then determined from the ratio between the concentrations in these two flows. Due to the standard error in chromatographic measurement, low values of X could therefore carry some uncertainty. Measurements were then done at least in triplicate by alternating the samplings of entrance and exit flows.

Considering various dead volumes in the set-up, running the experiment for several hours was necessary to attain a stationary feed. Monitoring the experiment over 5 days under

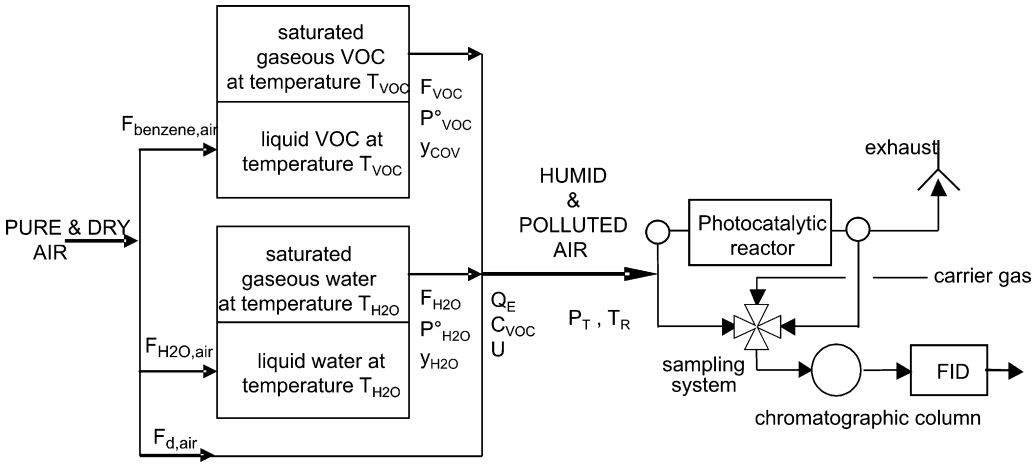

Fig. 1. Diagram of the experimental set-up.

typical conditions, during which the standard deviation for the entrance and exit concentration was of about 2%, satisfactorily validated the stability of the system.

Alternatively, the reactor exit flow was analysed so as to monitor CO and CO_2. To this effect, the chromatograph temperature was set to 30 °C and the flow at the exit of the chromatographic column was allowed to pass through a catalytic microreactor of methanation consisting in 0.401 g of homemade catalyst (18.5% in weight of Ni on alumina) at a temperature of 300 °C. The methanised flow was then allowed to enter the FID detector so as to measure the methane formed. Calibrating measurements permitted to check that the methanation was complete.

The identification of the intermediates has been carried out with a mass spectrometer MS agilent 5973 Network Mass selective detector coupled with a gas phase chromatograph agilent 6850 series with a DB5 MS column.

3. Kinetic measurement

3.1. Standard working conditions

Experiments were carried out under the following working conditions: in all experiments:

- catalyst load with respect to the support apparent surface: 2 mg cm^{-2},
- temperature T_R = 30 °C,
- total incident light flux $F^\circ = 1.28 \times 10^{-8}$ photons mol cm^{-2} s^{-1} (i.e. 4.19 mW cm^{-2}),

depending on the experiment:

- total flow rate Q = 50–300 mL min^{-1},
- benzene molar fraction C = 50–400 ppm (i.e. 50–400 ppmV),
- relative humidity H = 10–30%.

3.2. Measuring the rate of reaction

Although the intrinsic catalytic rate is usually expressed relatively to the amount of catalyst, the intrinsic rate r (mol min^{-1} m^{-2}) used in this study is expressed relative to the support apparent surface area. This is a more practical property, as the activity of the catalyst is mainly dictated by the irradiation flux per unit of support apparent area F°. Such an intrinsic rate thus depends on the catalyst thickness and the irradiation flux. Note that the catalyst deposit remained the same throughout the present study.

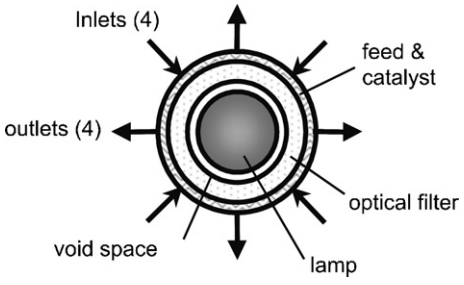

Fig. 2. Annular reactor (cross section).

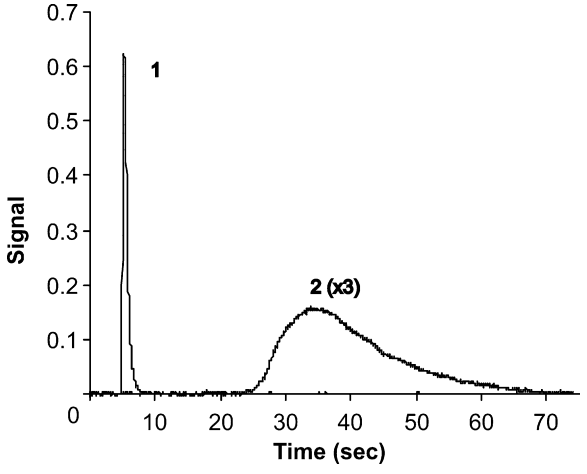

Fig. 3. Determination of residence time distribution (volume flow rate 200 mL min^{-1}): (1) input signal, and (2) output signal.

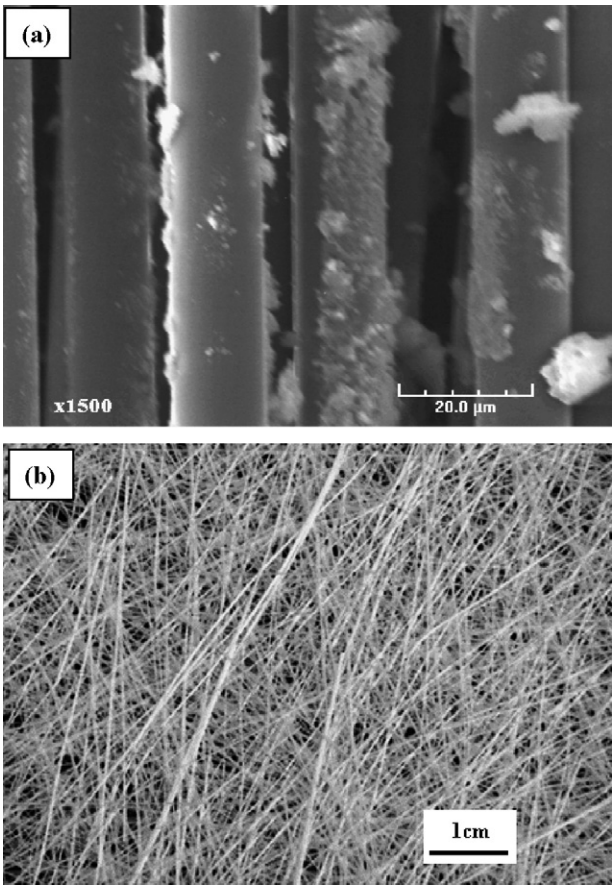

Fig. 4. (a) Optical picture of catalyst coated fibreglass support; (b) SEM picture of individual catalyst coated fibres.

The average rate is given from the mass balance by the following equation:

$$r(\text{mol min}^{-1}\,\text{m}^{-2}) = \frac{XF_{\text{VOC}}}{S} \quad (1)$$

where F_{VOC} is the VOC molar flow rate at the entrance of the reactor, as determined above, X the conversion yield and S is the catalyst support apparent surface area.

In a differential reactor, at low conversion yield, this average rate corresponds to the real rate under the entrance feed conditions. Such a moderate conversion could be ensured by a sufficient total volume flow rate. At high conversion yield, the data were analysed taking an integration into account (see below).

The role of mass transfer, internal or external, has been discussed in a previous study and found to be of negligible influence under the present conditions.

4. Kinetic results and discussion

4.1. Preliminary results

A first study [14] using a low titania deposit showed that the effect of benzene concentration on the rate of degradation did not follow a conventional Langmuir–Hinshelwood (LH) mechanism as it was the case for other VOCs such as trichloroethylene and methanol. This effect was attributed to a deactivation of the catalyst as already suggested [5–7,16]. This deactivation is fully apparent as the white catalyst becomes yellow and even brownish over an extensive period of use such as already observed [6–9]. It was very difficult to identify the nature of the products on the surface as they were very resistant to common organic solvents. With acetone and ether as solvent, the intermediates phenol and 4-hydroxy, 4-methyl, 2-pentanone have been identified. These intermediates were found in the colorless extract and therefore, were not at the origin of the coloration of the catalyst such as demonstrated before [5,7]. Other intermediates such as hydroquinone, benzoquinone [7] as well as catechol, resorcinol and oxalic acid [16] have been already identified. An IR analysis by DRIFT suggested a variety of chemical functions on the surface but none of them appeared as characteristic of a main chemical species. The colour itself could suggest the possibility of a quinonic compound. Moreover, no organic product could be detected in the gas phase by the chromatographic technique.

In order to study this deactivation process, the present study was carried out using a high amount of catalyst so as to follow the course of the deactivation. Experiments carried out on a fresh catalyst did agree with the LH mechanism as shown in Fig. 5 by following the apparent law as already observed [10,13,17,18]:

$$r = k_{deg}\frac{K_{\text{LH}}C}{1 + K_{\text{LH}}C} \quad (2)$$

K_{LH} is the adsorption constant, C the benzene molar fraction in the gas phase and k_{deg} a kinetic constant. In these experiments, the yield of conversion was high (X>50%) so that the kinetics parameters were determined by integration over the reactor. The mass balance can be written as:

$$r\text{d}S = -Q\,\text{d}C \quad (3)$$

with dS the differential apparent surface area of the catalyst support, Q the total volume flow rate and dC the variation of the

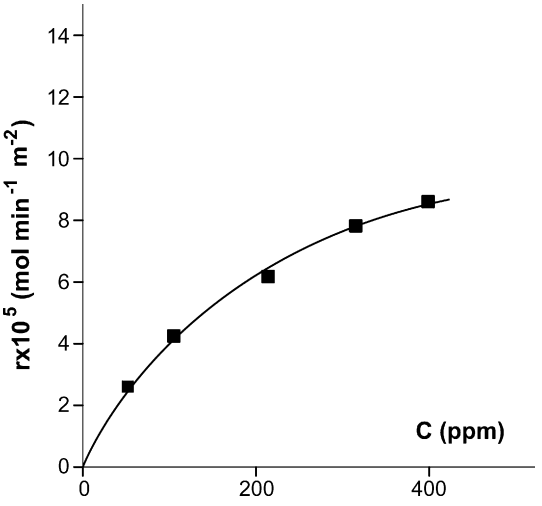

Fig. 5. Effect on benzene molar fraction on the rate of degradation on a clean catalyst (standard conditions, Q = 300 mL min^{-1} and H = 10%).

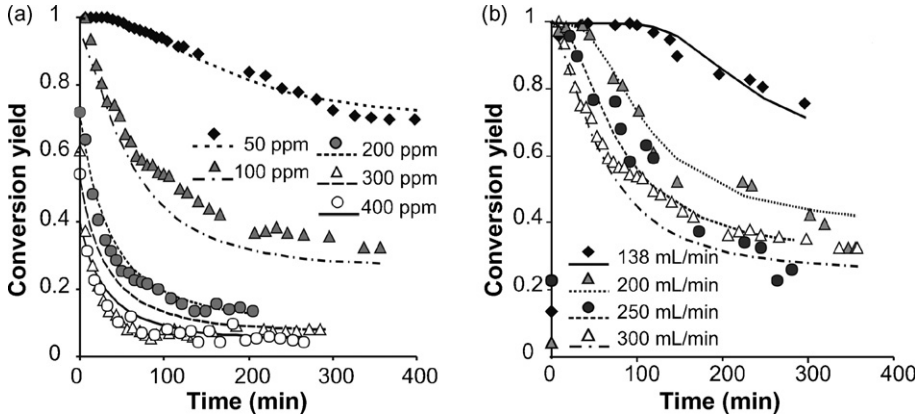

Fig. 6. (a) Yield of conversion of benzene as a function of time at constant total volume flow rate (300 mL min^{-1}) for various molar fractions of benzene in the feed; (b) idem at constant total molar fraction of benzene in the feed (100 ppm) for various total volume flow rates. Recalculated values (lines) using the aggregates model and to fit these data on the conversion only.

concentration along dS. The following implicit law was then obtained:

$$\frac{1}{k_{deg}K_{LH}}\ln\left(\frac{Cs}{Ce}\right)+\frac{1}{k_{deg}}(Cs-Ce)=-\frac{S}{Q} \quad (4)$$

with Ce and Cs, respectively, the concentration of the inlet and the outlet of the reactor. From this experiment values of the parameters were $k_{deg}=0.13\times10^{-3}$ mol min^{-1} m^{-2} and $K_{LH}=9.5\times10^{-3}$ ppm^{-1}.

4.2. Catalyst deactivation and regeneration

However, when carrying the reaction on a long time, the activity was found to decrease towards a limiting value under various experimental conditions as shown in Fig. 6 where the phenomenon was followed by the decrease in the yield of conversion X. Note that in these experiments the residence time was about 13 s, whereas the evolution on X was followed on a larger time scale (several hours), which means that X represented the instantaneous state of efficiency of the photocatalytic reactor.

In addition, when the reactor was allowed to run without benzene in the feed (still maintaining the irradiation and the relative humidity) the catalyst activity was totally recovered after regeneration time of about the same value as the deactivation time. The ''clean'' catalyst mentioned above in Fig. 5 was obtained by this treatment. Most authors have repeatedly observed this phenomenon [6–9]. Einaga et al. [8] have found that the amount of carbon deposits on the catalyst surface increases with increasing benzene concentration.

The chemical monitoring of the deactivation and regeneration phases was carried out by measuring the molar fraction of CO and CO_2 in the exit flow as shown in Fig. 7. The decrease in the production of CO and CO_2 and in the conversion of benzene during the deactivation phase suggests a decrease in the number of the actives sites on the catalyst surface. This can be due to the accumulation of strongly adsorbed intermediates on the surface.

4.3. Carbon balance

The degradation of benzene and the formation of carbon oxides were compared over a full experiment, that is over the

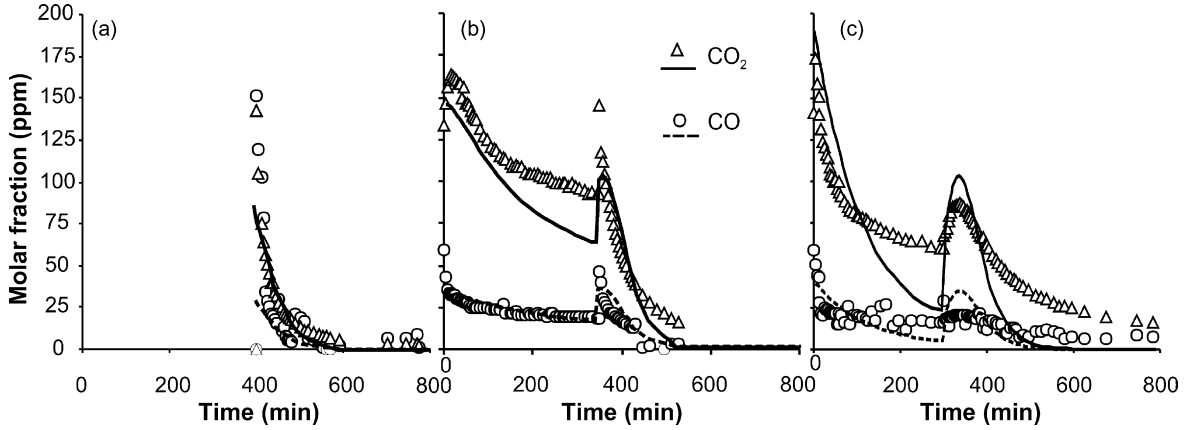

Fig. 7. Variation of the molar fraction of CO and CO_2 as a function of time at the reactor exit during the regeneration phase. $Q=300$ mL min^{-1}, $H=10\%$; (a) $C=50$ ppm, deactivation phase 400 min, (b) $C=100$ ppm, deactivation phase 350 min, (c) $C=300$ ppm, deactivation phase 300 min. Recalculated values (lines) using the aggregates model to fit both the conversion and CO, CO_2 concentrations data.

Table 1
Carbon balance during the deactivation and regeneration phases

Benzene (ppm) HR 10% during deactivation phase	Reaction time (h)	Relative humidity (%) during regeneration phase	Total CO and CO_2 products (mol)/*C* from benzene converted (mol)		Total (%)
			Deactivation phase (%)	Regeneration phase (%)	
300	3.5	10	53	43	96
		20	53	44	97
		30	53	41	94
100	5	10	58	39	97
300	5	10	47	48	95

deactivation phase and the regeneration, so as to check the carbon balance (see Table 1). Integrating the molar fractions in CO and CO_2 led to an integral $I_{CO_x}(D)$ and $I_{CO_x}(R)$ for the deactivation and regeneration phases, respectively, and integration of the disappeared benzene $C(1-X)$ over the deactivation phase (no benzene during the regeneration phase) led to the integral I_B. The ratio $I_{CO_x}(D)/6I_B$ corresponding to the deactivation phase was found to be lower than the unity, but the ratio over the total experiment $\{I_{CO_x}(D) + I_{CO_x}(R)\}/6I_B$ was found to close the unity. This shows that benzene is partially degraded during the exposition to the catalyst leading to CO and CO_2 and one or several intermediates strongly adsorbed and that the remaining intermediates are degraded on the catalyst during the second phase into carbon oxides. The accumulation of the intermediates are then responsible for a decrease in the activity of the catalyst during the deactivation phase but after a complete cycle of deactivation and regeneration all the carbon species are therefore degraded and the activity of the catalyst is recovered. The stoichiometry of the oxidation reaction can be written (at least for the carbon balance) roughly as:

$$C_6H_6 + O_2 = xCO + (6-x)\,CO_2 + (3\,H_2O?) \quad (5)$$

with a value of x of about 1.5.

5. Reactor modelling

5.1. Basic modelling

The present model is developed so as to get the benzene conversion and the molar fraction of CO and CO_2 at the exit of the reactor as a function of time, for a given molar fraction of benzene in the entrance flow. It is designed on two levels:

- A kinetic level where the reaction rates are determined as a function of benzene molar fraction and abundance in resistant intermediate according to the chosen mechanism and associated reaction parameters.
- A reactor level where the local balance in benzene, CO, CO_2 and resistant intermediate are determined at time t using the rates given above; this allows us to determine the concentration of these species along the reactor and in particular the flow composition at the exit.

The comparison of this calculated flow composition at the exit with experimental data shown in Figs. 6a, b and 7a–c allows the best fitting kinetic parameters to be determined and the validity of the model to be checked.

5.2. Basic kinetic model

The basic kinetic model is based on several assumptions:

- Taking into account that the LH mechanism is followed on a clean catalyst, the benzene is considered to adsorb on the surface according to a Langmuir model and the adsorption process is considered to be at the thermodynamic equilibrium.
- Adsorbed benzene is assumed to undergo a photocatalytic degradation (according to the LH mechanism) so as to give CO, CO_2 and a resistant intermediate as product.
- The intermediate is assumed to be irreversibly adsorbed and only removed by its photocatalytic degradation, giving CO, CO_2 as products and possibly another resistant intermediate and so on, the final degradation leading to CO and CO_2.
- Benzene adsorption only takes place on the sites which are unoccupied by the intermediates: the abundance of these intermediates is responsible for the loss in activity in the course of the deactivation phase.

As CO and CO_2 appear immediately during the deactivation phase, there are amongst the products of initial degradation of benzene. The appearance of CO and CO_2 during the regeneration phase implies that there are also the products of degradation of the resistant intermediate(s).

According to a simplified scheme, CO and CO_2 should appear in the elementary reactions of degradation, with integer stoichiometric coefficients. However, it was found difficult to obtain a satisfactory simulation with this constraint. Accordingly, the stoichiometric coefficients were optimized and do not have an integer value. Such a fact can be interpreted by the concept that the proposed mechanism is simplified and is a rough image of a more complicated reaction scheme with several processes which would all respect the constraint of realistic integer stoichiometric coefficients. Note that the same is often thought of the LH mechanism, which would be an apparent mechanism, convenient for its simplicity although not rigorous.

Variations in the model described in the following result from whether there are one (for the sake of simplification) or more intermediates and from the type of kinetic law followed by the photocatalytic degradation of the intermediate.

5.3. Calculation

In this ''integral reactor'', the benzene molar fraction C depends on the position along the catalyst bed. Assuming a plug-flow reactor, only one parameter is necessary, which is the distance 1 from the entrance. In addition, the catalyst undergoes a progressive deactivation so that C is not only a function of l but also of time t starting at $t = 0$ when the benzene is injected in the feed. For the same reasons, the extent of deactivation and the molar fraction of CO or CO_2 are functions of l and t.

Solving of the double differential system can be carried out by separating l and t variables.

Assuming that the reaction of benzene is fast, a quasi-stationary state of $C(l,t)$ can be written at a given time t. Then, the mass balance during δt, in a slice of reactor between l and $l + \delta l$, is written as:

$$10^6 F_E C(l,t)\delta t = r_B \frac{Z\,dl}{l^\circ}(1-\theta_I(l,t))\delta t + 10^6 F_E\, C(l+\delta l,t)\delta t \quad (6)$$

where F_E (mol min^{-1}) is the total molar flow at the reactor entrance (supposed to be practically constant throughout the reactor considering the low molar fraction of the reactants and products), Z (mol) the total number of sites on the catalyst, l° (m) the length of the reactor and r_B (min^{-1}) the rate of reaction of benzene for a clean surface expressed as a turn-over number and θ_I the surface coverage of the sites by the deactivation species (so that only the fraction of surface $(1 - \theta_I)$ is available to benzene adsorption and degradation).

According to a LH mechanism, r_B is expressed as:

$$r_B = k_B\left[\frac{K_{LH}C(l,t)}{(1+K_{LH}C(l,t))}\right] \quad (7)$$

where k_B (min^{-1}) is a rate constant, K_{LH} (ppm^{-1}) the adsorption constant of benzene.

Considering the simple case of a single intermediate, the balance in resistant intermediate in the same slice of reactor between the times t and $t + \delta t$ can be written as:

$$\frac{Z\,dl}{l^\circ}\theta_I(l,t+\delta t) = \frac{Z\,dl}{l^\circ}\theta_I(l,t) + r_B\frac{Z\,dl}{l^\circ}(1-\theta_I(l,t))\delta t - r_I\frac{Z\,dl}{l^\circ}\theta_I(l,t)\delta t \quad (8)$$

where r_I is the rate of degradation of the intermediate expressed as a turn-over number.

This is equivalent to (8bis):

$$\theta_I(l,t+\delta t) = \theta_I(l,t) + r_B(1-\theta_I(l,t))\delta t - r_I\theta_I(l,t)\delta t \quad (8bis)$$

In Eq. (8), the rate of degradation of the intermediate is assumed to be proportional to the surface coverage as in the conventional LH mechanism.

The appearance of CO and CO_2 results from the degradation of the benzene and of the intermediate so that the balance in the slice of reactor during the interval δt is written (with the subscript $x = 1$ or 2 for CO or CO_2, respectively):

$$10^6 F_E C_{COx}(l+\delta l,t)\delta t = 10^6 F_E\, C_{COx}(l,t)\delta t + \nu_{B,COx} r_B \frac{Z\,dl}{l^\circ}(1-\theta_I(l,t))\delta t + \nu_{I,COx} r_I \frac{Z\,dl}{l^\circ}\theta_I(l,t)\delta t \quad (9)$$

where ν_{B,CO_x} and ν_{I,CO_x} are the stoichiometric coefficients of CO_x produced in the reaction degradation of the benzene or of the intermediate, respectively.

In the calculation the initial conditions are:

- $C(0,t) = C$ during the deactivation phase,
- $C(0,t) = 0$ during the regeneration phase,
- $C(l,0) = 0$,
- $\theta_I(l,0) = 0$.

The calculation is carried out step by step over l and t alternatively so as to get the resulting molar fractions at the exit of the reactor in the course of the reaction $C(l^\circ,t)$, $C_{CO}(l^\circ,t)$ and $C_{CO_2}(l^\circ,t)$, as long as the conversion yield $X = [C(0,t) - C(l^\circ,t)]/C(0,t)$ during the deactivation phase.

This result depends on the value of a set of parameters, which are to be chosen:

- k_B, K_{LH}, r_I and Z, which permit to calculate X,
- the four stoichiometric coefficients ν_{B,CO_x} and ν_{I,CO_x} for $x = 1$ and 2 in order to calculate the molar fractions of CO and CO_2 at the exit of the reactor.

5.4. Extension of the model

The basic model accounts well for the variations of the conversion yield, but not for a maximum in the formation of CO_2 during the regeneration phase. Therefore, this basic model had be modified accordingly. Models based on two types of sites, as already suggested [10,13,17,18], do not account for this maximum. A simple extension of the model would be to consider the formation of two successive intermediates. However, when tested, this extended model gave a poor fit so that an alternative model was developed. This model was based on the formation of aggregates of a single intermediate (representing all types of intermediates present on the surface).

If the resistant intermediate tends to accumulate as aggregates on the surface, its degradation will depend on the extent of the periphery of the aggregates and not on the extent of their area. At low coverage, the rate of degradation is low as there is little intermediate, at high coverage, there is a large quantity of intermediate but the periphery is small so, that the rate of degradation is low again and at medium coverage the rate of degradation goes though a maximum.

This model requires an expression of the length of the periphery of the aggregates as a function of the surface coverage. An analogy can be made with the formulation of Mampel [19] of the rate of an heterogeneous reaction occurring on the surface of a solid reactant, especially in the case of a

two-dimensions geometry. In Mampel's model, the periphery A (per unit of surface area) can be found to be:

$$A(\theta) = \frac{9\pi r_g}{G}^{1/3} [-\ln(1-\theta)]^{2/3}(1-\theta) \quad (\mathrm{m}^{-1}) \tag{10}$$

where r_g is the rate of germination ($\mathrm{min}^{-1}\ \mathrm{m}^{-2}$) and G the rate of growth of the germs ($\mathrm{m\ min}^{-1}$).

This expression cannot be applied strictly to the present case as r_g cannot be defined and G is not constant, but it can be used to estimate the value of $A(\theta)$, and therefore r_I to a multiplicative factor. It can be shown also that the exponent 2/3 on the logarithm becomes 1 when considering the case of a constant number of germs, which seems to be more representative of the present phenomenon. On the whole, the rate of degradation r_I could be written (as a turn-over number):

$$r_I = \frac{k_I[-\ln(1-\theta_I)]^n(1-\theta_I)}{\theta_I} \tag{11}$$

with a rate constant k_I (min^{-1}) (to be adjusted) and an exponent n to be chosen between 2/3 and 1.

This expression of r_I was therefore used in Eq. (8bis).

5.5. Best-fitting parameters

The best-fitting parameters were determined using the SIMPLEX [20] method so as to minimize the difference between experimental data xe_i and calculated values xc_i. Basically this difference was expressed as the sum $X^2 = \Sigma(xe_i - xc_i)^2$ for the experimental points being considered. However, when considering simultaneously different experimental data such as the conversion and the CO or CO_2 concentrations these X^2 terms were of a different order of magnitude. In order to carry a global best-fitting over several sets of various data, a relative function X_r^2 was calculated for each of the sets, defined as $X_r^2 = X^2/xe_m^2$ where xe_m was the mean value of the xe_i data. The function to be minimized was then taken as the sum of the terms X_r^2 determined for each of the sets of experimental data. This allowed the different sets to have a comparable weight in the optimization process. As the calculated values xc_i are linear functions of the stoichiometric coefficients for CO and CO_2, these coefficients could be calculated algebraically from various summations.

6. Results of the modelling

6.1. Analysis at constant relative humidity

In a first step, only the benzene conversion X was taken into account in order to check the validity of the model. The data consisted in the variations of X with time for various feed concentrations and flow rates as shown in Fig. 6. Satisfactory recalculations of X using the aggregate model were obtained within the experimental error. These are plotted in the same figure with the following parameters:

- $Z = 6.7 \times 10^{-5}$ mol
- $K_{LH} = 4.7 \times 10^{-2}\ \mathrm{ppm}^{-1}$
- $k_B = 3.6 \times 10^{-2}\ \mathrm{min}^{-1}$
- $k_I = 2.0 \times 10^{-2}\ \mathrm{min}^{-1}$
- $n = 3/4$ (not a sensitive parameter).

Note that the value obtained for Z is coherent with the estimation of a theoretical value of 1.5×10^{-4} mol based on the total covering of the surface. The adsorption constant K_{LH} somewhat differ from the value determined above at short times. The two values are of the same order of magnitude and it must be pointed out that the value of this parameter is not very sensitive in the best fitting process.

In a second step, CO and CO_2 concentrations at the exit were taken into account. A best fitting based on these experimental data only, led to a satisfactory result but the parameters Z and the stoichiometric coefficients for CO and CO_2 had aberrant values. Carrying the best fitting with the conversion data and CO, CO_2 concentrations was then necessary. This led to a satisfactory global result (see Fig. 7), although the recalculation of conversion data was slightly less good as it is in Fig. 6.

6.2. Effect of relative humidity

All data represented in Figs. 6 and 7 were obtained with a constant relative humidity H of 10%. The effect of varying H is shown in Fig. 8 in the case of the conversion X during the deactivation phase and in Fig. 9 for the formation of CO and CO_2 during the regeneration phase. As shown in Fig. 8, the increase in H led to a decrease in X at short times and an increase in X at long times. The effect at short times suggests that a competitive adsorption of water and benzene takes place, which reduces benzene adsorption and therefore the rate of degradation. On the contrary, the degradation of the intermediate is much favoured by the presence of water, especially when considering the effect of H on the formation of CO and CO_2 during the regeneration phase as shown in Figs. 8 and 9. Water has indeed been already found to favour the degradation of benzene [6,8,9,21,22].

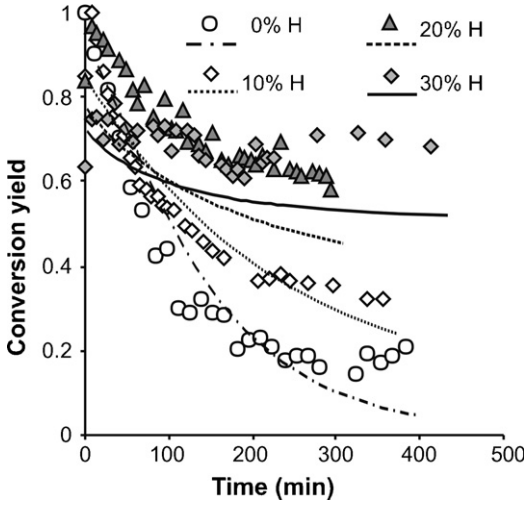

Fig. 8. Variations of the conversion with the irradiation time for a variable relative humidity 0, 10, 20, 30% ($Q = 300$ mL min^{-1}, and $C = 100$ ppm). Recalculated values (lines) to fit all data.

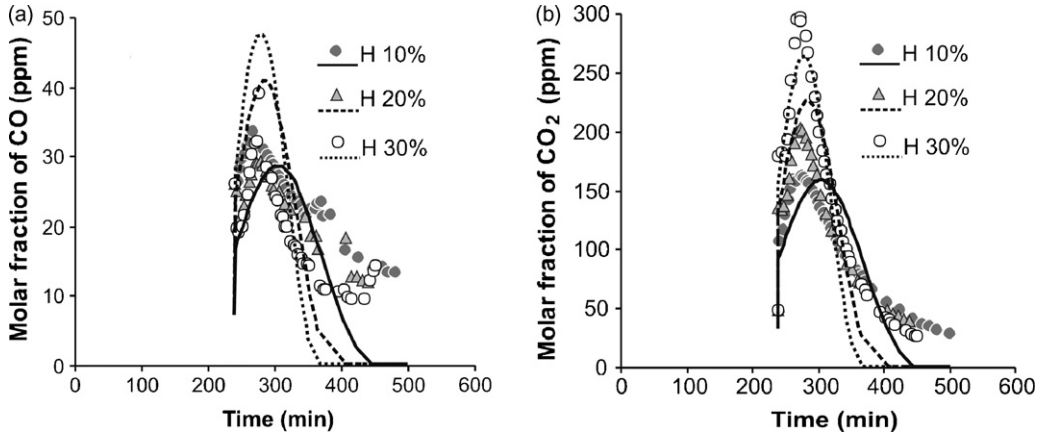

Fig. 9. Variations of the CO, CO_2 concentrations during the recovering phases for $H = 10$, 20, 30% ($Q = 150$ mL min^{-1}, deactivation phase $C = 300$ ppm, 4 h). Recalculated values (lines) to fit all the data.

This has been taken into account in the view of introducing the water concentration in the model. The effect of competitive adsorption is simply represented by a simple Langmuir model where the coverage by benzene molecules is expressed as in (12) instead of (7):

$$r_B = k_B \left[\frac{K_{LH} C(l,t)}{1 + K_{LH} C(l,t) + K_W C_W} \right] \quad (12)$$

where K_W and C_W are the constant of adsorption and the concentration of water, respectively.

It is assumed here that C_W remains constant throughout the reactor and is independent on time on the basis of a water concentration much higher than benzene concentration and therefore a small consumption of water during the residence time in the reactor.

As shown in Fig. 8, the benzene conversion takes place, although slowly, in the absence of water. This suggests that water is not a necessary reactant to convert benzene into the intermediate. A possibility is an initial process in the form of a direct reduction of the aromatic ring by holes of the photocatalyst. The rate constant k_B was therefore considered to be independent of the water concentration C_W.

The increase in intermediate degradation induced by water suggests that water is the source of reactive hydroxyl radicals able to attack organic molecules, a mechanism generally thought as the most active in photocatalysis. This was simply taken into account by considering that the concentration of hydroxyl radicals on the surface and therefore the rate photocatalytic reaction was proportional to the water coverage. The rate of intermediate degradation was then rewritten as in Eq. (13) instead of Eq. (11):

$$r_I = k_I [-\ln(1-\theta_I)]^n \left[\frac{(1-\theta_I)}{\theta_I} \right] \left[\frac{K_W C_W}{1 + K_{LH} C(l,t) + K_W C_W} \right] \quad (13)$$

This model including the effect of water was applied to the best fitting of the whole set of data leading to the calculated plots in Figs. 8–11. Although reconstruction is imperfect, the general trend is satisfactorily represented using the model. The following parameters were found:

- $Z = 1.8 \times 10^{-4}$ mol,
- $K_{LH} = 6.7 \times 10^{-2}$ ppm^{-1},
- $K_W C_W = 0.67$ (for a relative humidity H of 10%),

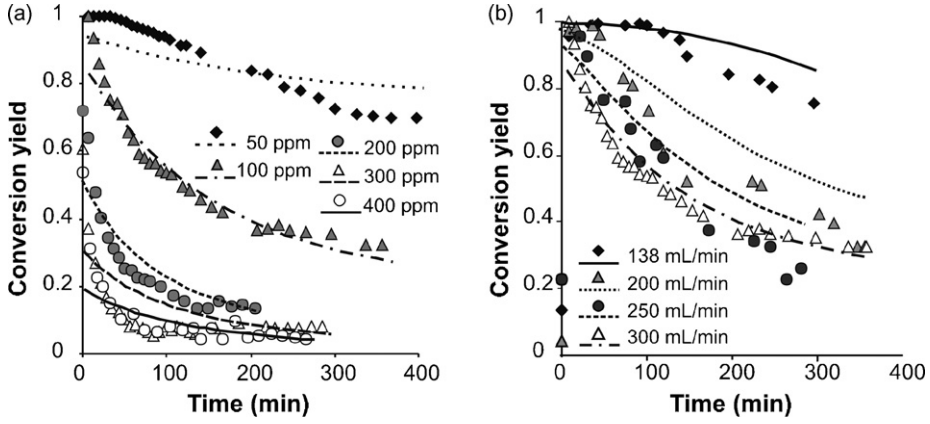

Fig. 10. (a) As Fig. 6a (b) Fig. 6 b. Recalculated values (lines) using the aggregates model to fit all the data.

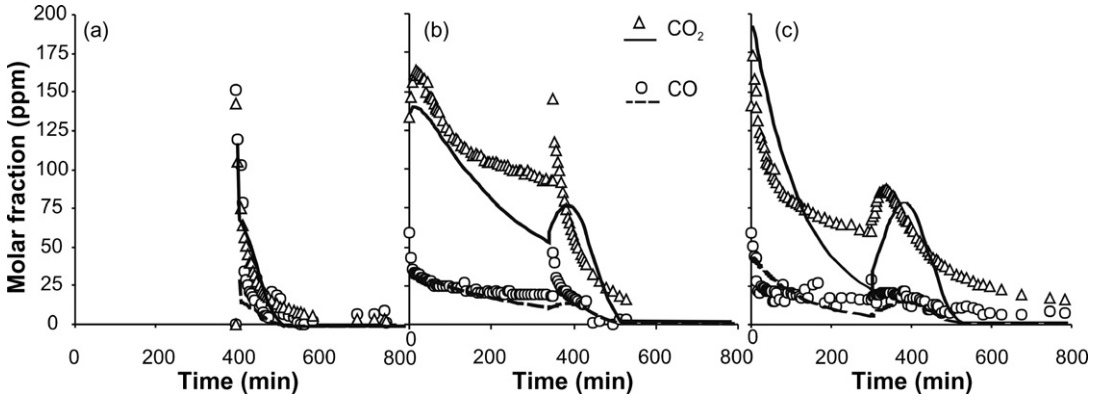

Fig. 11. As in Fig. 7 a, b. Recalculated values (lines) using the aggregates model to fit all the data.

- $k_B = 1.0 \times 10^{-3}$ min^{-1},
- $k_I = 4.3 \times 10^{-2}$ min^{-1},
- $n = 3/4$ (not a sensitive parameter).

The value of Z slightly exceeds the maximum estimated value but the actual value does not have a strict significance, this only means that most sites are involved in the process of adsorption.

The total stoichiometric coefficients for CO and CO_2 formation were of about 0.5 for CO and 2.5 for CO_2. Although the ratio between these two coefficients is coherent with the general stoichiometric Eq. (5), the calculated values are about half the expected values. The discrepancy takes its origin mainly in the absence of CO and CO_2 at long times in regeneration phase where the concentrations are low but persist for a long time. The model finds therefore its validity mainly in the short times when the burst of CO and CO_2 formation is observed.

7. Conclusion

The photocatalytic degradation of benzene has proved complex and takes place though the formation of resistant intermediates which occupy the surface and progressively deactivate the photocatalyst. However, these intermediates are themselves degraded so that the conversion of benzene tends to reach a photostationary value. In the absence of benzene, the activity of the catalyst can be totally restored. The degradation of the intermediate is efficiently favoured by water so that the photostationary deactivation is much reduced for a relative humidity of 30%. On the contrary, water does not appear to be of importance in the primary attack of benzene itself. A kinetic model has been proposed which takes into account a deactivation in the form of intermediate aggregates, which are degraded on their periphery. Considering these speculative aggregates, the general trend of the reaction during a deactivation and regeneration phase is then satisfactorily represented with a few parameters. This model can help in the design of a photoreactor for the treatment of benzene.

Acknowledgement

The authors thank the LSGC for allowing the use of the RTD set-up and for SEM pictures.

References

[1] O. Legrini, E. Oliveros, A.M. Braun, Chem. Rev. 93 (1993) 671.
[2] D.F. Ollis, H. Al Ekabi, Photocatalytic Purification and Treatement of Water and Air, Elsevier Science Publisher, Amsterdam, 1993.
[3] J.M. Hermann, Catal. Today 24 (1995) 157.
[4] M.R. Hoffmann, S.T. Martin, W. Choi, D.W. Bahnemann, Chem. Rev 95 (1995) 69.
[5] S.A. Larson, J.L. Falconer, Catal. Lett. 44 (1997) 57.
[6] H. Einaga, S. Futamura, T. Ibusuki, Appl. Catal. B: Environ. 38 (2002) 215.
[7] O. d'Hennezel, P. Pichat, D.F. Ollis, J. Photochem. Photobiol. A 118 (1998) 197.
[8] H. Einaga, S. Futamura, T. Ibusuki, Phys. Chem. Chem. Phys. 1 (1999) 4903.
[9] N.N. Lichtin, M. Sadeghi, J. Photochem. Photobiol. A 113 (1998) 81.
[10] M. Lewandowski, D.F. Ollis, Appl. Catal. B 45 (2003) 223.
[11] H. Einaga, S. Futamura, T. Ibusuki, Environ. Sci. Technol. 35 (2001) 1880.
[12] Lewandowski, D.F. Ollis, J. Catal. 217 (2003) 38.
[13] M. Lewandowski, D.F. Ollis, Appl. Catal. B: Environ. 43 (2003) 309.
[14] N. Doucet, F. Bocquillon, O. Zahraa, M. Bouchy, Chemosphere 65 (2006) 1188.
[15] O. Zahraa, C. Dorion, S.M. Ould-Mame, M. Bouchy, J. Adv. Oxid. Technol. 4 (1999) 40.
[16] W.A. Jacoby, D.M. Blake, J.A. Fennell, J.E. Boulter, L.M. Vargo, M.C. George, S.K. Dolberg, J. Air Waste Manage. Assoc. 46 (1996) 891.
[17] T.N. Obee, Environ. Sci. Technol. 30 (1996) 3578.
[18] T.N. Obee, R.T. Brown, Environ. Sci. Techno. 29 (1995) 1223.
[19] W.H. Press, B.P. Flannery, S.A. Teukolsky, W.T. Vetterling, Numerical Recipes, Cambridge University Press, Cambridge, 1986, p. 289.
[20] D. Barret, Cinétique hétérogène, Gauthier-Villards, Paris, 1973, p. 283.
[21] J.F. Wu, C.H. Hung, C.S. Yuan, J. Photochem. Photobiol. A: Chem. 170 (2004) 299.
[22] S. Sitkiewitz, A. Heller, New J. Chem. 20 (1996) 233.